nature geoscience

ARTICLES

PUBLISHED ONLINE: 25 APRIL 2010 | DOI: 10.1038/NGEO843

Towards inferring earthquake patterns from geodetic observations of interseismic coupling

Yoshihiro Kaneko[1]*, Jean-Philippe Avouac[2] and Nadia Lapusta[2,3]

Ultimately, seismotectonic studies seek to provide ways of assessing the timing, magnitude and spatial extent of future earthquakes. Ample observations document the spatial variability in interseismic coupling, defined as a degree of locking of a fault during the period of stress build-up between seismic events: fully or nearly locked fault patches are often surrounded by aseismically creeping areas. However, it is unclear how these observations could help assess future earthquakes. Here we simulate spontaneous seismic and aseismic fault slip with a fully dynamic numerical model. Our simulations establish the dependence of earthquake rupture patterns and interseismic coupling on spatial variations of fault friction. We consider the long-term evolution of slip on a model fault where two seismogenic, locked segments are separated by an aseismically slipping patch where rupture is impeded. We find that the probability for a large earthquake to break through the rupture-impeding patch is correlated with the interseismic coupling averaged over this patch. In addition, the probability that an earthquake breaks through the rupture-impeding patch and interseismic coupling are both related to fault friction properties through a single non-dimensional parameter. Our study opens the possibility of predicting seismic rupture patterns that a fault system can produce on the basis of observations of its interseismic coupling, and suggests that regions of low interseismic coupling may reveal permanent barriers to large earthquakes.

Simple conceptual models of fault behaviour assume that seismic rupture segmentation is persistent and that fault segments remain locked in the interseismic period separating episodic slip events[1]. These models predict quasiperiodic repetition of 'characteristic' earthquakes with similar rupture extent and moment[2] or a time-predictable or slip-predictable behaviour if non-quasiperiodic behaviour is allowed[1]. As observations accumulate, it becomes quite evident that earthquake sequences on natural faults are more complex than these simple models predict[3–6], although faults do seem to obey some systematic behaviours with respect to their segmentation[7] and, possibly, the timing of major earthquakes[8]. One potential explanation is that faults may consist of several subsegments that rupture either independently or jointly with neighbouring segments during larger earthquakes[7,9], with the non-periodic or even chaotic behaviour arising from stress transfers and their effect on prestress[10–12]. This segmentation may partly be controlled by geometrical complexities such as local non-planarity and fault step-overs[13]. However, there is growing evidence that spatial variation of fault friction properties is an influential and perhaps determining factor that affects the spatial extent, size and timing of earthquake ruptures. Hence, barriers prone to aseismic creep may have an important effect on the observed patterns of seismic ruptures, an issue that is the focus of this study.

Evidence for heterogeneous fault friction properties

Measurements of surface deformation show that, in the interseismic period between successive large earthquakes, some fault areas remain locked whereas others creep aseismically. This has been observed along a number of subduction zones including Sumatra, Japan, Alaska, Peru and Chile[14–19]. The pattern of interseismic coupling (ISC), the ratio of slip deficit during the interseismic period divided by the long-term slip (Supplementary Information S2), is thus generally found to be heterogeneous and, to some degree, coincides with the pattern of large earthquakes. For example, the distribution of seismic asperities in the Kurile–Japan trench seems to be relatively stationary[20] and lie within a zone with high ISC (ref. 21). Similarly, large earthquakes offshore of Sumatra seem to have ruptured areas that had remained locked during the interseismic period[6,16]. More evidence that the mode of slip on faults varies spatially comes from observations of aseismic afterslip occurring in areas surrounding the seismic ruptures[19,22–25] and seismic patches embedded in creeping faults in various tectonic settings[15,26,27].

These observations can be interpreted as evidence for heterogeneous fault friction properties. In the laboratory, both rock surfaces and layers of fault gouge have been shown to exhibit rate and state frictional behaviour (Supplementary Information S1), in which the steady-state frictional strength τ_{ss} can be expressed as[28,29]

$$\tau_{ss} = \bar{\sigma}\left[f_0 + (a-b)\ln(V/V_0)\right] \quad (1)$$

where a and b are rate and state parameters, V is slip rate, f_0 and V_0 are the reference friction coefficient and slip rate and $\bar{\sigma}$ is the effective normal stress. In steady state, rock friction exhibits either velocity weakening (VW, $a-b<0$) or velocity strengthening (VS, $a-b>0$), depending on a number of factors including normal stress, temperature and the type of rock material[28–32]. Models predict that VS fault regions would slip stably under slow tectonic loading, whereas VW fault regions would produce 'stick–slip' motion[12,33–38].

In this framework, earthquakes and aseismic slip are mainly linked to VW and VS segments, respectively, although earthquakes can penetrate into VS segments and parts of VW segments can

[1]Institute of Geophysics and Planetary Physics, Scripps Institution of Oceanography, University of California, La Jolla, California 92093, USA, [2]Division of Geological and Planetary Sciences, California Institute of Technology, Pasadena, California 91125, USA, [3]Division of Engineering and Applied Science, California Institute of Technology, Pasadena, California 91125, USA. *e-mail: ykaneko@ucsd.edu.

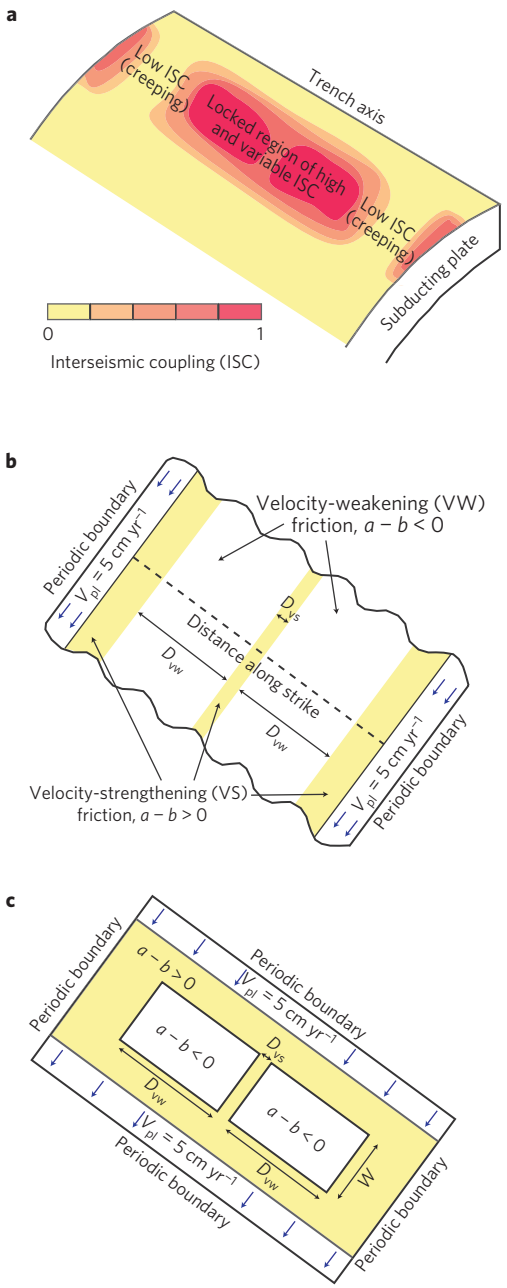

Figure 1 | Schematic illustrations of ISC as commonly observed on subduction megathrust faults and distribution of friction properties in our 2D and 3D models. a, The proportion of slip accommodated by interseismic creep varies spatially, from 0% in fully locked areas (ISC = 1) to 100% in areas creeping with the interplate rate (ISC = 0). **b**, The 2D model is intended to investigate the effect of friction heterogeneity in the along-strike direction. **c**, The 3D model has the same along-strike heterogeneity of friction properties at the seismogenic depth as the 2D model but incorporates a finite seismogenic fault width W.

experience aseismic slip[37,39–41]. Fault patches that creep aseismically can be interpreted to be dominantly VS whereas locked patches are dominantly VW. Predominantly creeping patches that are characterized by a VS frictional behaviour can act as systematic barriers to earthquake propagation, as in the case of the Batu Islands area, Sumatra[16], or in the Paracas Peninsula area, Southern Peru[19]. On the other hand, some earthquakes rupture across aseismic barriers. For example, the 1964 Alaska earthquake of moment magnitude M_w 9.2 ruptured through an area with locally low ISC (ref. 42). The impeding effect of this patch may have been responsible for the two-peaked source-time function[43]. Similarly, the 2007 Pisco earthquake ruptured two locked patches separated by a VS barrier[19,44]. Patches with relatively low ISC, but not as pronounced as in the Batu Islands, are also observed in the Mentawai Islands[16] and presumably influenced the 2007 earthquake sequence[6]. The non-systematic effect of these heterogeneities on seismic ruptures might be the origin of the complex behaviour of this area, which repeatedly involved clustered large earthquakes with overlapping rupture areas[8]. Together, these observations imply that spatial variations of fault friction properties can influence the location and extent of seismic ruptures in a systematic or non-systematic manner. However, how such variations translate into the pattern of ISC and complexity of earthquake ruptures is not well understood. To explore this issue, we construct fault models that contain variations in friction properties.

Model of earthquake cycles with heterogeneous coupling

We use numerical experiments to explore the effect of VS patches on ISC and on the seismic rupture pattern over many earthquake cycles. Our model contains a planar fault governed by the ageing form of rate and state friction[28,29] and embedded in a homogeneous elastic medium (Supplementary Information S1). The fault has two identical VW segments separated and surrounded by VS regions. In the simpler two-dimensional (2D) implementation, we consider only along-strike variations (Fig. 1b), which enables us to assess a broad range of model behaviour as the parameters are varied. Several calculations in a three-dimensional (3D) model (Fig. 1c) are conducted to check the validity of the findings derived from the 2D simulations. The fault is loaded by imposing a constant slip velocity outside the simulated region. The friction properties and lengths of the fault segments are varied to study their effect on the model behaviour. Fault slip is simulated using a unique methodology[37,45] that resolves all stages of seismic and aseismic slip: the aseismic nucleation process, the subsequent inertially controlled earthquakes with realistic slip rates and rupture speeds, the postseismic slip and the interseismic deformation between earthquakes.

Realistic earthquake behaviour produced by the model

Despite the simple geometry and distribution of friction properties, the model produces rich earthquake behaviour similar to that of natural faults. A 2D simulation example is shown in Fig. 2 (Supplementary Movie S1 gives a 3D simulation example). The VW segments are nearly fully locked in the interseismic period (ISC $\approx$ 1) and slip mostly during seismic events. Some earthquakes rupture only a fraction of a VW segment (for example, events 3–5 in Fig. 2b); they arrest because of lower prestress caused by previous slip (Fig. 3). Other events grow large and sometimes propagate through the VS patch. The large VS regions of low ISC on both sides of the model act as permanent barriers to coseismic slip. The central VS patch affects local ISC and acts as a barrier during some coseismic ruptures (for example, events 6, 14 and 25 in Fig. 2b). In the example of Fig. 2, 83% and 10% of the total slip in the VS patch is accumulated seismically and as afterslip, respectively (Fig. 2f). This example shows that a region of nearly uniform and high ISC can have significant variations in friction properties, resulting in complex rupture patterns (Fig. 2).

The VS patch causes clustering of large events and overlapping rupture areas. When only one of the VW segments ruptures, stress is transferred to the neighbouring VW segment owing to the coseismic static stress change and afterslip, leading to event clustering: the two VW segments tend to rupture much closer in time than their recurrence periods (Fig. 2c). After such one-segment ruptures, stress increase in the VS patch promotes propagation of the subsequent large earthquake through the patch. The slightly VS patch gradually relieves the transient stress

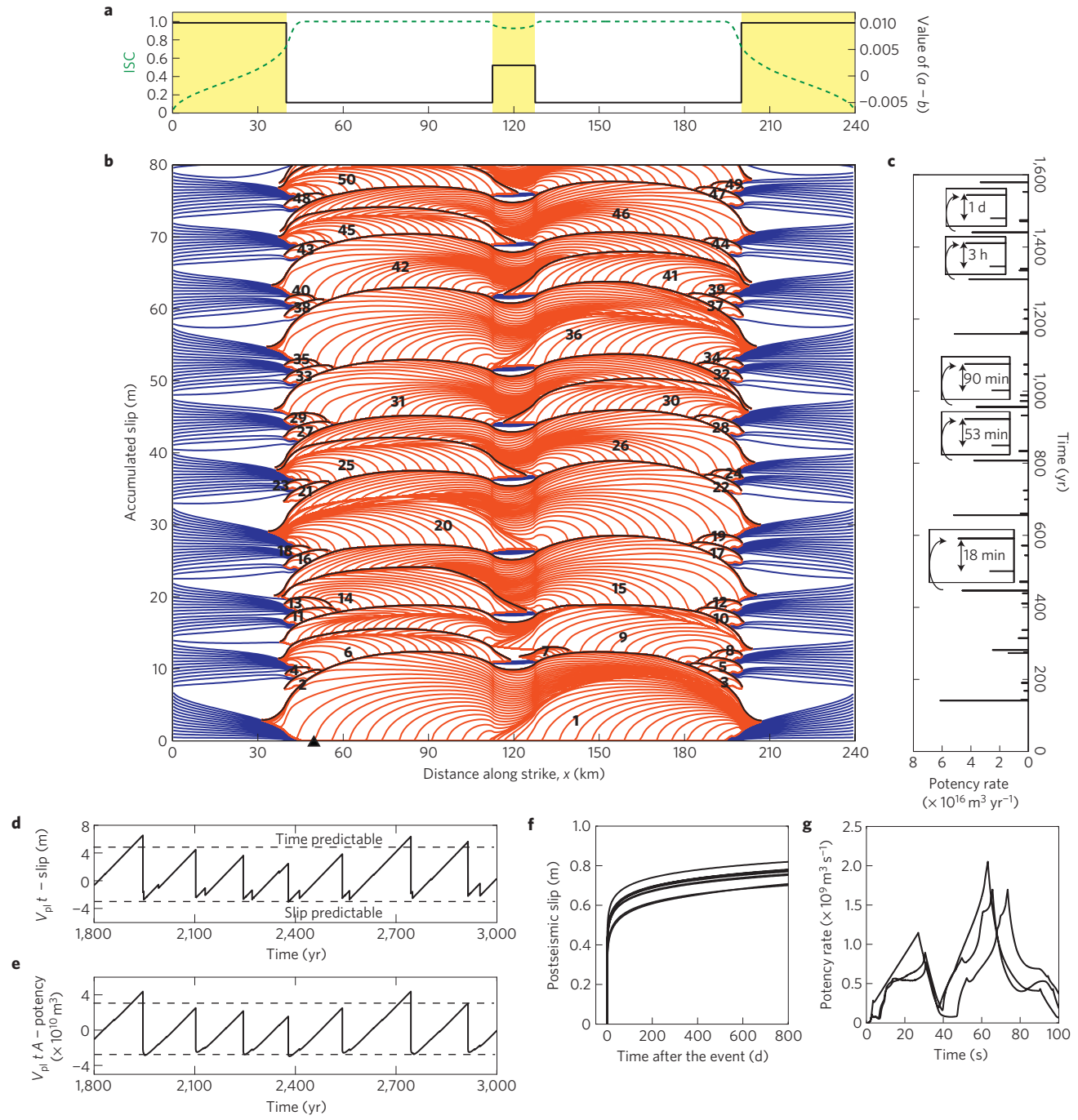

Figure 2 | An example of long-term fault behaviour computed in the 2D model. a, The assigned distribution of the friction parameter ($a-b$) (solid line) results in a small VS patch between two VW segments, which appear as a single area of high and slightly variable ISC (dashed line) (Supplementary Information S2). In this example, the VS patch results in a locally lower ISC, but the effect is subtle (ISC = 0.93). **b**, Contours of slip accumulated over 1,600 yr show that the VS patch creates complexity of large earthquakes within what seems to be a locked area of high ISC. Red, blue and black lines show slip accumulation every 2 s during the simulated earthquakes, every 10 yr and after each earthquake, respectively. Numbers indicate earthquakes in the order of their occurrence. **c**, Potency rate over time (a downdip width of 40 km is assumed). Insets show close-up views of clustered successive events. **d**, Time evolution of slip deficit at one VW point ($x = 50$ km) indicated by a triangle in **b**. Dashed lines illustrate that the model is neither time nor slip predictable. **e**, Potency deficit over the entire fault. **f**, Afterslip computed at the centres of the VS patch ($x = 120$ km) after events 1, 9, 15, 20, 26, 31, 36 and 42, which all propagated through the VS patch. **g**, Potency rates of events 1, 20 and 36 show that the VS patch results in double-peaked source-time functions.

increase by afterslip, but the stress level often remains high at the time of the next large earthquake, promoting rupture propagation through the patch. Hence a VS patch within a well-locked zone can be identified as a place where nearby ruptures tend to overlap, with the second rupture being generally larger than the first one. For example, event 6 (Fig. 2b) ruptures only the left VW segment and then event 9 is able to rupture both VW segments eight years later. This behaviour may explain the overlapping rupture areas of the 1797 M_w 8.8 and 1833 M_w 9.0 earthquakes in Sumatra.

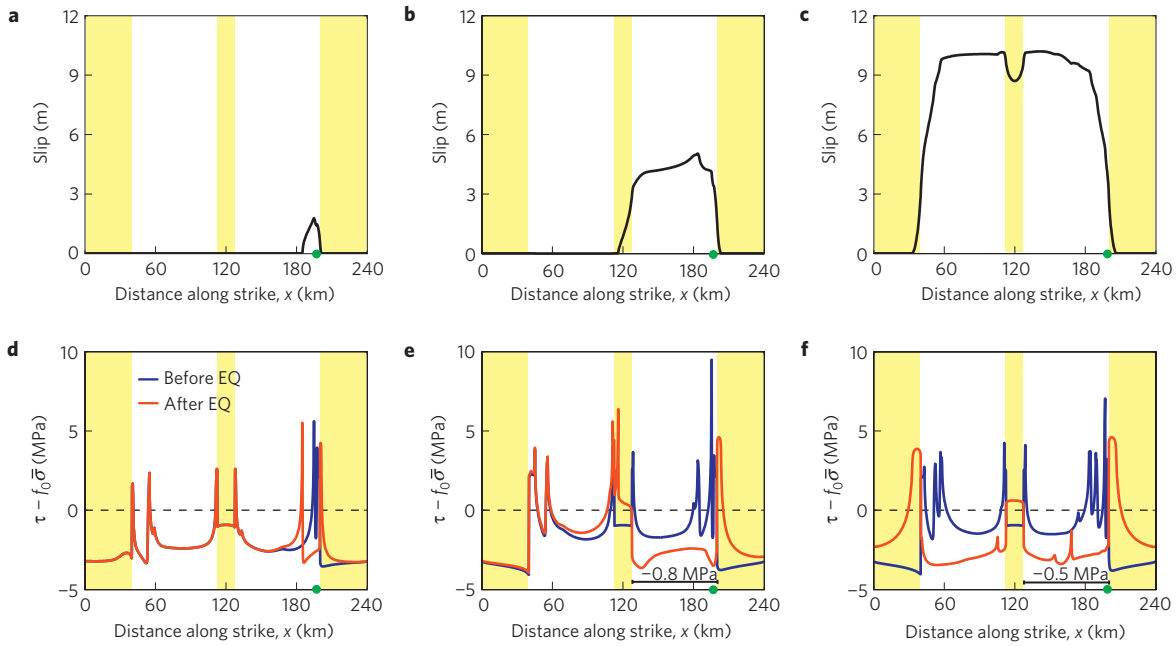

Figure 3 | Characteristics of simulated earthquakes and causes of rupture arrest. a–c, Coseismic slip distributions for three representative, earthquakes (events 28, 30 and 36 in Fig. 2b) including an event that arrests in the VS patch (**b**) and an event that propagates through the patch (**c**). **d–f**, The corresponding distributions of shear stress τ before and after the earthquakes, with respect to a reference stress value $f_0\bar{\sigma}$. We define the beginning/end of an earthquake as the time when the maximum slip rate V_{max} on the fault reaches/decreases below 1 cm s^{-1}. Epicentres are marked by green dots. Coseismic static stress drops are in the range of 1–10 MPa, typical for natural earthquakes.

For a wide range of parameters, our model does not produce characteristic earthquakes, nor does it obey the slip-predictable or the time-predictable behaviour at a given point on the fault (Fig. 2d). The model does not exhibit the time-predictable behaviour because the model does not incorporate a fixed threshold shear stress for slip to occur. The behaviour is closer to being slip predictable, even more so if the average slip (or equivalently the slip potency) is considered rather than slip at one particular point (Fig. 2e). This is because, after each earthquake, the shear stress on the ruptured area drops to the same level, approximately determined by the steady-state friction equation (1) evaluated at the coseismic slip rate $V = V_{dyn}$ (~1–10 m s^{-1}). The simulations also show that assessing whether the fault exhibits time- or slip-predictable behaviour requires an extended history with many earthquake cycles.

Quantifying the effect of VS patches on seismic ruptures

The effect of the central VS patch on the resulting pattern of large earthquakes can be quantified in terms of the probability that an earthquake that has ruptured one VW segment would propagate through the VS patch, rupturing at least a part of the second VW segment. The probability is estimated from the percentage P of earthquakes that propagate through the VS patch relative to the number of earthquakes that rupture entirely one of the two VW segments.

Clearly, the larger the length D_{vs} of the VS patch and the higher the average stress increase $\Delta\tau_{prop}$ required for seismic slip within the VS patch, the smaller would be the percentage of earthquakes that propagate through the VS patch. An approximation for $\Delta\tau_{prop}$ can be obtained by considering the difference in average shear stress on the patch before and during seismic slip and a further contribution from the breakdown work[46], a quantity sometimes called fracture energy. Hence we define the resistance C of the VS patch as (Supplementary Information S3)

$$C = \Delta\tau_{prop} D_{vs} = \bar{\sigma}_{vs}(a_{vs} - (1-\lambda^*)b_{vs})\ln\left(V_{dyn}/V_i\right)D_{vs} \qquad (2)$$

where the subscript 'vs' refers to the parameters characterizing the VS patch, $0 \le \lambda^* \le 1$ accounts for breakdown work at the crack tip, and V_{dyn} and V_i are the representative seismic slip velocity and slip velocity at the end of the interseismic period on the VS patch. The values of V_{dyn} and V_i depend on the model behaviour, but their variation is limited in our simulations. V_{dyn} is of the order of the typical seismic slip velocity of 1 m s^{-1}, and V_i ranges from the plate velocity of 10^{-9} m s^{-1} to values smaller by 1–2 orders of magnitude, so that $\ln(V_{dyn}/V_i) \approx 20$, nearly independent of the model parameters. Inclusion of parameter λ^* is only important for patches with friction properties close to velocity neutral (Supplementary Information S3). Hence, for most cases, the patch resistance (equation (2)) can be approximated by $C_{appr} = 20\bar{\sigma}_{vs}(a_{vs} - b_{vs})D_{vs}$.

This is exactly what our simulations show (Fig. 4a). In simulations with a broad range of patch parameters D_{vs} and $\bar{\sigma}_{vs}(a_{vs} - b_{vs})$, the percentage P of two-segment ruptures is approximately constant for the same value of C_{appr} (Fig. 4a). Smaller values of C_{appr} enable nearly every rupture to propagate through the VS patch, larger values result in the patch acting as a permanent barrier and intermediate values allow for a rich behaviour with comparable numbers of earthquakes arresting and propagating through the patch as in the case of Fig. 2.

The properties of VW segments also significantly affect probability P. Rupture of a VW segment increases stress on the VS patch, and the larger the stress increase, the larger P is expected to become. The stress increase can be represented (Supplementary Information S3) as $\beta\Delta\tau_{vw}D_{vw}$, where $\Delta\tau_{vw}$ is the average stress drop over the VW segment, D_{vw} is the length of the VW segment and β is a model-dependent geometric factor between 0 and 1. For the 3D model, both the patch resistance and the transferred stress need to be multiplied by the seismogenic fault width W. We use $\beta = 1/2$ for the 2D model and $\beta = W/(2D_{vw} + 2W)$ for the 3D model. This is based on the assumption that stress is transferred equally in all directions and that, in 3D models, β is proportional to the perimeter of the VW segment that is contiguous with the VS patch.

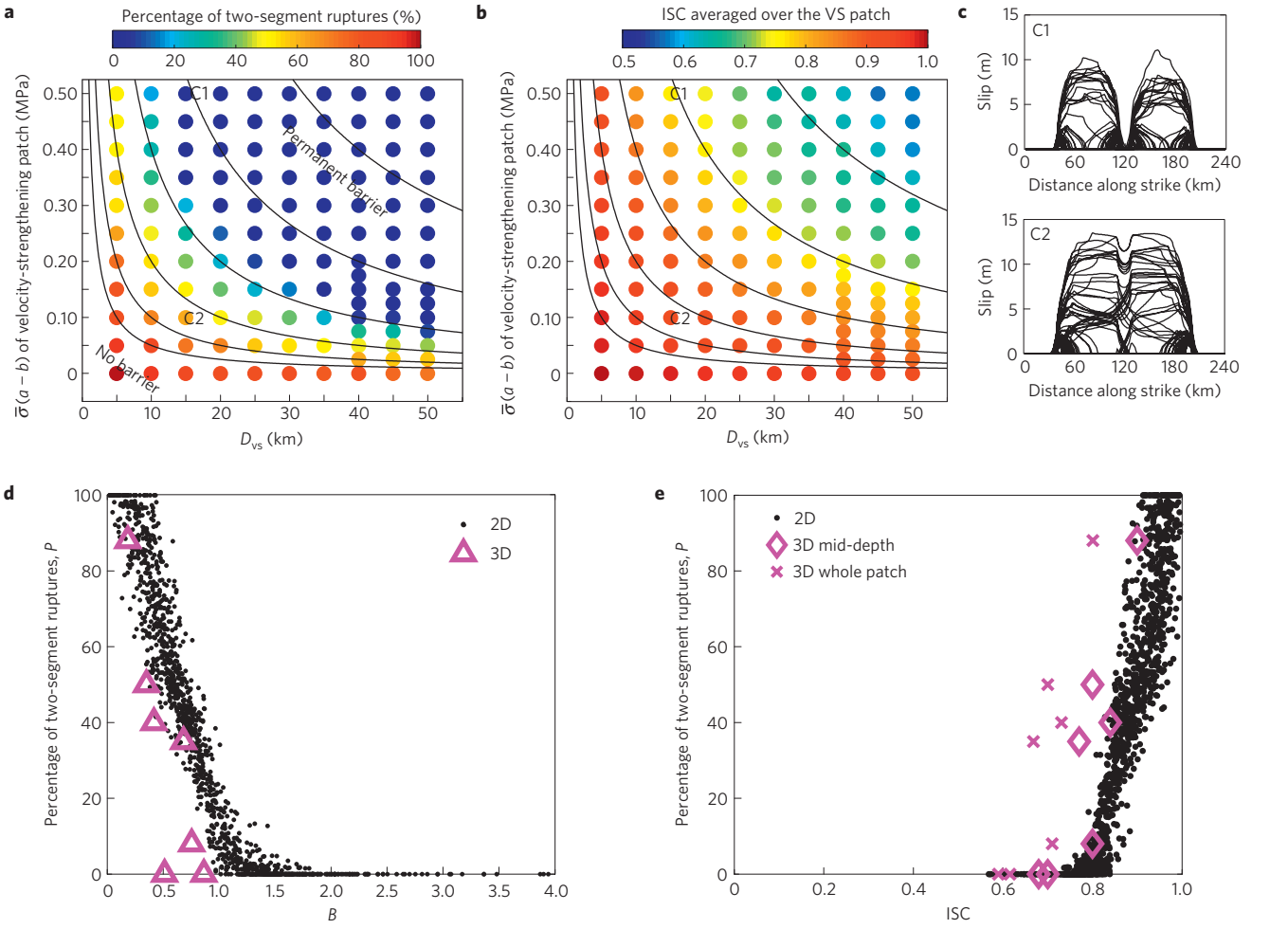

Figure 4 | Relation between the properties of VS and VW regions, probability *P* that an earthquake would propagate through the VS patch, and ISC. **a**,**b**, Properties of the VS patch have a similar systematic effect on both the pattern of seismic ruptures, as quantified by *P*, and ISC averaged over the patch. $P = 0\%$ corresponds to a permanent barrier. Each colour of dot represents a 2D simulation of 9000 yr of fault slip, with more than 50 events that rupture either one or both VW segments. Isocontours of $\bar{\sigma}(a_{vs} - b_{vs})D_{vs}$ (solid lines) pass through similar values of *P* and ISC in **a** and **b**, respectively. Properties of the VW segments are the same for all cases. **c**, Slip distributions of events corresponding to cases C1 and C2 illustrate the range of model behaviour. The VS patch can either act as a permanent barrier (C1) or enable most of the earthquakes to propagate through (C2), despite being of the same size. **d**, Relation between *P* and non-dimensional parameter *B* for several 3D simulations and a large set of 2D simulations in which the properties of both VW and VS regions are systematically varied (Supplementary Table S1). All results collapse, with some scatter, onto a single curve. **e**, The percentage *P* of two-segment ruptures and ISC averaged over the VS patch are closely related. The labels '3D mid-depth' and '3D whole patch' correspond to ISC averaged over the mid-seismogenic depth and over the entire VS patch, respectively.

The barrier efficiency of a VS patch can thus be characterized with the non-dimensional parameter:

$$B = \frac{\Delta\tau_{prop} D_{vs}}{\beta \Delta\tau_{vw} D_{vw}} \quad (3)$$

which can be approximated by $B_{appr} = (20\bar{\sigma}_{vs}(a_{vs} - b_{vs})D_{vs})/(\beta\Delta\tau_{vw}D_{vw})$ for most cases. The larger the *B* value, the smaller should be the percentage of ruptures that propagate through the patch. Figure 4d shows that *P* is indeed correlated with *B* (equation (3)) for a large number of simulations in which we have varied the properties and sizes of the VW and VS segments, and the effective normal stress (Supplementary Table S1). This plot demonstrates that *B* is an appropriate parameter to quantify the effect of the VS patch on the pattern of large earthquakes. The results of 2D and 3D models collapse nearly onto the same curve in Fig. 4d, showing that parameter *B* can be used to connect the results of the 2D model to the more realistic 3D situations. This also means that, for the same characteristics of the VW and VS regions that enter *B*, the VS patch acts as a stronger barrier in the 3D model, because the value of β is smaller for the 3D model (1/6 for the particular geometry used, with $W = D_{vw}/2$).

Relation of ISC to rupture patterns and individual events

Our simulations indicate that the size and friction properties of the VS patch influence ISC similarly to the effect on earthquake ruptures (Fig. 4). ISC decreases as either D_{vs} or $\bar{\sigma}_{vs}(a_{vs} - b_{vs})$ increases, with the ISC being approximately the same for a constant value of their product C_{appr} (Fig. 4b). For a wide range of model parameters, we find that ISC in the VS patch correlates with the percentage *P* of earthquakes rupturing through it (Fig. 4e). This has an important implication for seismic hazard because the rupture extent of large earthquakes is linked to variations in ISC. This conclusion holds for both 2D and 3D simulations. Note that, for the same percentage *P* of two-segment ruptures, ISC is lower in the 3D simulations, because there the VS patch is directly loaded by the adjacent larger VS regions that creep at nearly the plate loading rate. Regardless of the model or how the values of ISC

are computed, a VS patch with a locally lower, but still high, ISC (ISC $\lesssim 0.6$) can systematically arrest coseismic ruptures (Fig. 4e). This means that a VS patch compensates for the deficit in seismic slip not through a significant decrease in ISC, but rather through significant postseismic slip after events that stop near the patch.

The correlation between ISC and earthquake patterns characterized by P is not surprising. Accumulated slip must be relatively uniform over the fault domain and equal to the sum of co-, post- and interseismic slip. It follows that the overall seismic behaviour of the VS patch is related to the amount of cumulative slip occurring in the interseismic period, and hence to ISC. The correlation between ISC and P implies that ISC also depends on the non-dimensional parameter B. In fact, it can be shown that ISC and B_{appr} are related in a spring–slider model for cases when the patch acts as a permanent barrier (Supplementary Information S4).

We observe that the source-time function of earthquakes that rupture through a VS patch contains multiple peaks (Fig. 2g), the phenomenon commonly inferred from inversions of large earthquakes[6,43,44]. This is because both the potency rate and rupture speed first decrease as rupture propagates through the central VS patch and then increase after the rupture front enters the neighbouring VW segment. However, a multiple-peaked source-time function could also arise owing to a region of lower prestress on a VW fault (sometimes referred to as an 'anti-asperity'). The two types of heterogeneity can be distinguished from postseismic observations, because afterslip would occur within a VS patch (Fig. 2f) but not within a VW region of lower prestress. Thus, variations in seismic potency rates combined with the distribution of postseismic slip can be used to infer smaller-scale heterogeneities in friction properties within a locked region of high but variable ISC.

Towards quantitative seismic hazard assessment

This study demonstrates that friction heterogeneities provide a unifying explanation for a variety of observations of fault behaviour regarding individual ruptures, earthquake sequences and patterns of ISC. Fault areas with VS friction, which can be detected from geodetic or remote-sensing measurements of interseismic and postseismic strain, may be the primary cause for the relative persistence of seismic rupture segmentation and asperities. At the same time, the presence of such VS patches can explain other aspects of the long-term seismic behaviour of faults such as clustering of large events, overlapping of subsequent ruptures and ruptures of several locked segments. Our results suggest that relatively small VS patches could have a profound effect on the long-term seismic behaviour but a subtle effect on ISC.

The presented work provides physical insights into how spatial heterogeneities in fault friction properties—observed through seismic, postseismic and interseismic slip—can influence future earthquakes. Thus, our study opens up ways to make quantitative use of geodetic and seismic observations for seismic-hazard assessment. This study focuses on large earthquakes on subduction megathrusts. However, our conclusions should be applicable to any environment and scale, including smaller scales, that contain heterogeneities in fault friction properties.

Received 10 February 2010; accepted 18 March 2010; published online 25 April 2010

References

1. Shimazaki, K. & Nakata, T. Time-predictable recurrence model for large earthquakes. *Geophys. Res. Lett.* **7,** 279–282 (1980).
2. Schwartz, D. P. & Coppersmith, K. J. Fault behaviour and characteristic earthquakes: Examples from the Wasatch and San Andreas fault zones. *J. Geophys. Res.* **89,** 5681–5698 (1984).
3. Schwartz, S. Y. Noncharacteristic behavior and complex recurrence of large subduction zone earthquakes. *J. Geophys. Res.* **104,** 23111–23125 (1999).
4. Murray, J. & Segall, P. Testing time-predictable earthquake recurrence by direct measurement of strain accumulation and release. *Nature* **419,** 287–291 (2002).
5. Weldon, R., Fumal, T. & Biasi, G. Wrightwood and the earthquake cycle: What a long recurrence record tells us about how faults works. *GSA Today* **14,** 4–10 (2004).
6. Konca, O. A. *et al.* Partial rupture of a locked patch of the Sumatra megathrust during the 2007 earthquake sequence. *Nature* **456,** 631–635 (2008).
7. Thatcher, W. Order and diversity in the modes of Circum-Pacific earthquake recurrence. *J. Geophys. Res.* **91,** 2609–2623 (1990).
8. Sieh, K. *et al.* Earthquake supercycles inferred from sea-level changes recorded in the corals of west Sumatra. *Science* **322,** 1674–1678 (2008).
9. Kanamori, H. & McNally, K. C. Variable rupture mode of the subduction zone along the Ecuador–Colombia coast. *Bull. Seismol. Soc. Am.* **72,** 1241–1253 (1982).
10. Rundle, J. B., Kanamori, H. & McNally, K. C. An inhomogeneous fault model for gaps, asperities, barriers and seismicity migration. *J. Geophys. Res.* **89,** 10219–10231 (1987).
11. Cochard, A. & Madariaga, R. Complexity of seismicity due to highly rate-dependent friction. *J. Geophys. Res.* **101,** 25321–25336 (1996).
12. Ariyoshi, K. *et al.* Character of slip and stress due to interaction between fault segments along the dip direction of a subduction zone. *J. Geodyn.* **48,** 55–67 (2009).
13. Wesnousky, S. G. Predicting the endpoints of earthquake ruptures. *Nature* **444,** 358–360 (2006).
14. Freymueller, J. T., Cohen, S. C. & Fletcher, H. J. Spatial variations in present-day deformation, Kenai Peninsula, Alaska, and their implications. *J. Geophys. Res.* **105,** 8079–8101 (2000).
15. Igarashi, T., Matsuzawa, T. & Hasegawa, A. Repeating earthquakes and interplate aseismic slip in the northeastern Japan subduction zone. *J. Geophys. Res.* **108,** 2249 (2003).
16. Chlieh, M., Avouac, J-P., Sieh, K., Natawidjaja, D. H. & Galetzka, J. Heterogeneous coupling of the Sumatran megathrust constrained by geodetic and paleogeodetic measurements. *J. Geophys. Res.* **113,** B05305 (2008).
17. Moreno, M. S., Klotz, J., Melnick, D., Echtler, H. & Bataille, K. Active faulting and heterogeneous deformation across a megathrust segment boundary from GPS data, south central Chile (36°–39° S). *Geochem. Geophys. Geosyst.* **9,** Q12024 (2008).
18. Hashimoto, C., Noda, A., Sagiya, T. & Matsu'ura, M. Interplate seismogenic zones along the Kuril–Japan trench inferred from GPS data inversion. *Nature Geosci.* **2,** 141–144 (2009).
19. Perfettini, H. *et al.* Aseismic and seismic slip on the megathrust offshore southern Peru revealed by geodetic strain. *Nature* (in the press).
20. Yamanaka, Y. & Kikuchi, M. Asperity map along the subduction zone in northeastern Japan inferred from regional seismic data. *J. Geophys. Res.* **109,** B07307 (2004).
21. Ito, T., Yoshioka, S. & Miyazaki, S. Interplate coupling in northeast Japan deduced from inversion analysis of GPS data. *Earth Planet. Sci. Lett.* **176,** 117–130 (2000).
22. Hsu, Y-J. *et al.* Frictional afterslip following the 2005 Nias–Simeulue earthquake, Sumatra. *Science* **312,** 1921–1926 (2006).
23. Miyazaki, S., Segall, P., Fukuda, J. & Kato, T. Space time distribution of afterslip following the 2003 Tokachi-oki earthquake: Implications for variations in fault zone frictional properties. *Geophys. Res. Lett.* **31,** L06623 (2004).
24. Baba, T., Hirata, K., Hori, T. & Sakaguchi, H. Offshore geodetic data conducive to the estimation of the afterslip distribution following the 2003 Tokachi-oki earthquake. *Earth Planet. Sci. Lett.* **241,** 281–292 (2006).
25. Johanson, I. A., Fielding, E. J., Rolandone, F. & Bürgmann, R. Coseismic and postseismic slip of the 2004 Parkfield earthquake from space-geodetic data. *Bull. Seismol. Soc. Am.* **96,** 269–282 (2006).
26. Rubin, A. M., Gillard, D. & Got, J-L. Streaks of microearthquakes along creeping faults. *Nature* **400,** 635–641 (1999).
27. Bourouis, S. & Bernard, P. Evidence for coupled seismic and aseismic fault slip during water injection in the geothermal site of Soultz (France), and implications for seismogenic transients. *Geophys. J. Int.* **169,** 723–732 (2007).
28. Dieterich, J. H. Time-dependent friction and the mechanics of stick–slip. *J. Geophys. Res.* **116,** 790–806 (1978).
29. Ruina, A. L. Slip instability and state variable friction laws. *J. Geophys. Res.* **88,** 10359–10370 (1983).
30. Blanpied, M. L., Lockner, D. A. & Byerlee, J. D. Frictional slip of granite at hydrothermal conditions. *J. Geophys. Res.* **100,** 13045–13064 (1995).
31. Marone, C. Laboratory-derived friction laws and their application to seismic faulting. *Annu. Rev. Earth Planet. Sci.* **26,** 643–696 (1998).
32. Dieterich, J. H. Applications of rate- and state-dependent friction to models of fault slip and earthquake occurrence. *Treat. Geophys.* **4,** 107–129 (2007).
33. Tse, S. & Rice, J. R. Crustal earthquake instability in relation to the depth variation of frictional slip properties. *J. Geophys. Res.* **91,** 9452–9472 (1986).

34. Rice, J. R. & Ruina, A. L. Stability of steady frictional slipping. *J. Appl. Mech.* **50,** 343–349 (1983).
35. Ben-Zion, Y. & Rice, J. R. Slip patterns and earthquake populations along different classes of faults in elastic solids. *J. Geophys. Res.* **100,** 12959–12983 (1995).
36. Tullis, T. E. Rock friction and its implications for earthquake prediction examined via models of Parkfield earthquakes. *Proc. Natl Acad. Sci. USA.* **93,** 3803–3810 (1996).
37. Lapusta, N., Rice, J., Ben-Zion, Y. & Zheng, G. Elastodynamic analysis for slow tectonic loading with spontaneous rupture episodes on faults with rate- and state-dependent friction. *J. Geophys. Res.* **105,** 23765–23789 (2000).
38. Hori, T., Kato, N., Hirahara, K., Baba, T. & Kaneda, Y. A numerical simulation of earthquake cycles along the Nankai trough, southwest Japan: Lateral variation in frictional property due to slab geometry controls the nucleation position. *Earth Planet. Sci. Lett.* **228,** 215–226 (2004).
39. Rice, J. R. Spatio-temporal complexity of slip on a fault. *J. Geophys. Res.* **98,** 9885–9907 (1993).
40. Boatwright, J. & Cocco, M. Frictional constraints on crustal faulting. *J. Geophys. Res.* **101,** 13895–13909 (1996).
41. Chen, T. & Lapusta, N. Scaling of small repeating earthquakes explained by interaction of seismic and aseismic slip in a rate and state fault model. *J. Geophys. Res.* **114,** B01311 (2009).
42. Suito, H. & Freymueller, J. T. A viscoelastic and afterslip postseismic deformation model for the 1964 Alaska earthquake. *J. Geophys. Res.* **114,** B11404 (2009).
43. Christensen, D. H. & Beck, S. L. The rupture process and tectonic implications of the great 1964 Prince William sound earthquake. *Pure Appl. Geophys.* **142,** 29–53 (1994).
44. Sladen, A. *et al.* Source model of the 2007 M_w 8.0 Pisco, Peru earthquake—implications for seismogenic behavior of subduction megathrusts. *J. Geophys. Res.* **115,** B02405 (2010).
45. Lapusta, N. & Liu, Y. Three-dimensional boundary integral modeling of spontaneous earthquake sequences and aseismic slip. *J. Geophys. Res.* **114,** B09303 (2009).
46. Tinti, E., Spudich, P. & Cocco, M. Earthquake fracture energy inferred from kinematic rupture models on extended faults. *J. Geophys. Res.* **110,** B12303 (2005).

Acknowledgements

This study was supported by the National Science Foundation (grant EAR 0548277) and Caltech Tectonics Observatory. This is Caltech Tectonics Observatory contribution no 130. Numerical simulations for this study were carried out on the CITerra Dell cluster at the Division of Geological and Planetary Sciences of the California Institute of Technology.

Author contributions

Y.K. designed the study, carried out and analysed the numerical experiments and wrote the paper. J-P.A. and N.L. analysed the numerical experiments and contributed to the concept development. All authors discussed the results and commented on the paper.

Additional information

The authors declare no competing financial interests. Supplementary information accompanies this paper on www.nature.com/naturegeoscience. Reprints and permissions information is available online at http://npg.nature.com/reprintsandpermissions. Correspondence and requests for materials should be addressed to Y.K.